

Fascinating Role of the Number of f Electrons in Dipolar and Octupolar Contributions to Quadratic Hyperpolarizability of Trinuclear Lanthanides-Biscopper Schiff Base Complexes

Antonino Gulino,^{*,†} Ignazio L. Fragalà,[†] Fabio Lupo,[†] Graziella Malandrino,[†] Alessandro Motta,[†] Alessia Colombo,[‡] Claudia Dragonetti,^{*,‡,§} Stefania Righetto,[‡] Dominique Roberto,^{‡,§} Renato Ugo,[‡] Francesco Demartin,[‡] Isabelle Ledoux-Rak,^{||} and Anu Singh^{||}

[†]Dipartimento di Scienze Chimiche, Università di Catania and INSTM UdR of Catania, Viale Andrea Doria 6, 95125 Catania, Italy

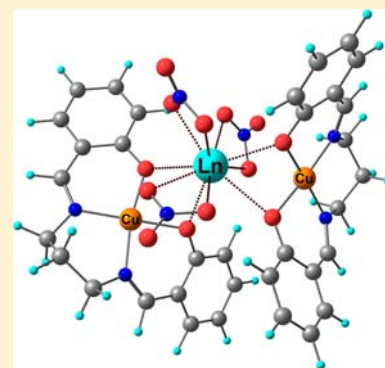
[‡]Dipartimento di Chimica, dell'Università degli Studi di Milano, UdR di Milano dell'INSTM, Milano, Italy

[§]Istituto di Scienze e Tecnologie Molecolari del CNR, Via Golgi 19, I-20133 Milano, Italy

^{||}Laboratoire de Photonique Quantique et Moléculaire UMR CNRS 8531 - Institut d'Alembert -, ENS Cachan, 61 avenue du Président Wilson, 94235 Cachan, France

S Supporting Information

ABSTRACT: The trinuclear $[\text{Ln}(\text{NO}_3)_3(\text{CuL})_2]$ complexes (Ln = La, Ce, Sm, Eu and Er, L = N,N'-1,3-propylen-bis(salicylideneiminato)) have been investigated by a combination of HLS and EFISH techniques to evaluate both the dipolar and octupolar contributions to their significant quadratic hyperpolarizability and to confirm that f electrons may tune their second-order NLO response. In the complexes investigated, the major contribution to the total quadratic hyperpolarizability is largely controlled by the octupolar contribution, but the values of both β_{EFISH} and $\|\beta^{f=1}\|$, that is the dipolar part, are significantly influenced by the number of f electrons, confirming that the unexpected polarizable character of f electrons may be the origin of such fascinating evidence.



INTRODUCTION

In the last two decades, organometallic and coordination complexes have emerged as new interesting molecular chromophores with second-order nonlinear optical (NLO) properties; in fact they may offer, when compared to traditional organic second-order NLO chromophores, additional electronic effects acting on the NLO response, such as charge-transfer transitions between the metal and the ligands (usually at low energy and high oscillator strength), tunable by virtue of the nature, oxidation state, and coordination sphere of the metal center.¹ For instance, coordination of a metal to second-order push-pull NLO π -delocalized nitrogen donor chromophores, bearing a strong electron-donor group, produces a significant increase of their NLO response, owing to a red-shift of the intraligand charge transfer transition (ILCT) induced by the metal acting as a Lewis acceptor. On the contrary, if the NLO chromophores bear a strong electron-acceptor group, the NLO response is mainly controlled by metal to ligand charge transfer transitions (MLCT).¹

Surprisingly, whereas lanthanide complexes have been intensively studied for their luminescent, magnetic, catalytic, and biological applications,² there are only a few reports on their rather unexpected second-order NLO properties.³ Le Bozec et al.^{3d,e} reported that dipolar $[\text{LLn}(\text{NO}_3)_3]$ (L =

dibutylaminophenyl-functionalized annelated terpyridine) complexes act as second-order NLO chromophores, with an increasing molecular quadratic hyperpolarizability, β_{HLS} , as measured by the Harmonic Light Scattering (HLS) technique, that parallels the increase in the number of f electrons. Similarly, the increase of β_{HLS} values of octupolar $\text{Na}_3[\text{Ln}(\text{pyridyl-2,6-dicarboxylate})_3]$ complexes along the Ln series was attributed to the increased number of f electrons.^{3f}

This dependency of the quadratic hyperpolarizability on the number of f electrons was rationalized by the polarization of the 4f electrons.^{3g}

This is rather unexpected since in the past, 4f levels in lanthanide compounds were considered essentially atomic in nature and simple spectators with respect to the chemical bond because filled 5s² and 5p⁶ levels shield 4f orbitals from significant ligand field effects.⁴ Although this certainly holds for ionic oxides and halogenated lanthanides,⁴ quantum mechanical calculation combined with photoelectronic spectroscopical studies highlighted some lanthanide-ligand covalency in discrete organometallic molecules.⁵ In addition, the experimental rationalization of the role of f electrons on the second-

Received: March 5, 2013

Published: June 19, 2013

order NLO properties made by Le Bozec et al.^{3d,e} has confirmed that 4f electrons may play a role in the hyperpolarizability outcome.

Besides, Tanner, Wong et al.^{3h} reported that the quadratic hyperpolarizabilities, determined by HLS technique, of various Ln complexes with nonadentate ligands based on triazacyclononane incorporating pyridyl-2-phosphinate groups reach a maximum around the center of the lanthanide series, with a bell-shaped trend. A similar peculiar trend of the second-order NLO response was observed by Parker et al.³ⁱ in the case of Ln complexes of *trans*-cinnamic acid; these latter two recent works witness how the interpretation of NLO data of the lanthanide complexes is extremely fascinating and of current interest.

Recently, some of us investigated⁶ the second-order nonlinear optical properties of various lanthanide (Ln) complexes [Ln(hfac)₃(diglyme)] (hfac = hexafluoroacetylacetonate; diglyme = bis(2-methoxyethyl)ether) by a combination of Electric-Field Induced Second Harmonic generation (EFISH) and HLS techniques, providing further evidence for the role of f electrons in tuning the second-order NLO response. Molecular quadratic hyperpolarizability values measured by the EFISH method, β_{EFISH} initially increase rapidly with the number of f electrons, whereas the increase is much lower for the last seven f electrons. The increase of β_{HLS} , which shows that the second-order NLO response is dominated by the octupolar contribution, is much lower along the Ln series.⁶

Copper(II)-lanthanide compounds with Schiff bases, known since the 1970s,⁷ are attracting attention also nowadays⁸ for their interesting magnetic properties, but, to our knowledge, surprisingly, their second-order NLO properties have never been investigated although Tiseanu^{8c} studied the one- and two-photon induced emission in Zn(II)–Sm(III) and Zn(II)–Tb(III) complexes with Schiff bases.

However, it is well-known that Schiff-bases, arising from condensation of substituted salicylaldehydes with various bridging diamines, represent suitable templates to generate second-order NLO-active noncentrosymmetric molecular architectures; for example, various bis(salicylaldiminato)M(II) (M = Fe, Co, Ni, Cu, Zn) complexes are efficient second-order NLO molecular chromophores.^{1d,9} Also, very recently, some of us reported an unprecedented switching of the second-order NLO response by addition of a Lewis base to aggregate bis(salicylaldiminato)zinc(II) Schiff-base complexes.¹⁰

Therefore these evidence prompted us to study the second-order NLO responses of trinuclear lanthanide adducts [Ln(NO₃)₃(CuL)₂] (Ln = La, Ce, Sm, Eu, and Er) with the N,N'-1,3-propylen-bis(salicylidiminato)copper(II) (CuL) coordinating as a bidentate ligand (see Figure 1) in order to investigate if, even in these more complex molecular architectures, there is evidence of the fascinating tunability by the number of 4f electrons.

EXPERIMENTAL SECTION

General Comments. We have used reagents as received from Sigma Aldrich for all syntheses. Elemental analyses were carried out in the Dipartimento di Chimica of the Università degli Studi di Milano. Infrared transmittance spectra were recorded using a Jasco FT/IR-430 spectrometer and the instrumental resolution was 2 cm⁻¹. Electronic absorption spectra have been obtained on a UV–vis V-650 Jasco spectrometer with a 0.2 nm resolution at room temperature. MALDI-TOF mass spectra were obtained on a Voyager DE-STR instrument (PerSeptive Biosystem) using a delay extraction procedure (25 kV applied after 2600 ns with a potential gradient of 454.54 V/mm and a wire voltage of 250 V) and detection in linear mode. The instrument

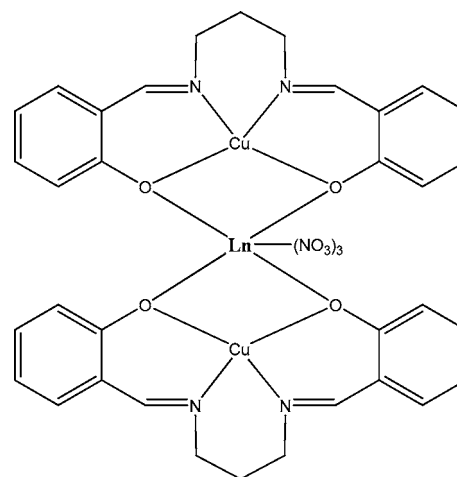


Figure 1. [Ln(NO₃)₃(CuL)₂] complexes.

was equipped with a nitrogen laser (emission at 337 nm for 3 ns, 50 Hz) and a flash AD converter (time base 2 ns). *trans*-3-Indoleacrylic acid was used as matrix. For MALDI measurements, the samples were dissolved in THF, mixed with the matrix, and loaded in the sample plate. Because of the isotopic composition, molecular species were detected in the mass spectra as clusters of peaks. The *m/z* values reported in the spectra and in the text are referred to the exact mass of the ion containing the most abundant isotope of each element present in the molecule.

Energy dispersive X-ray (EDX) measurements were performed to check the composition of the sample powders.

Computational Details. Dipole moments were calculated on the geometry-optimized structures using the G09 code¹¹ on CINECA cluster. The PBE approximation¹² was adopted for both exchange and correlation effect in the Density Functional Theory (DFT) framework with an open shell approach. The effective core potential (ECP) of Stuttgart/Dresden¹³ in the “small core” approximation (mwb) was employed for the lanthanide atoms (La, Ce, Sm, Eu, and Er) to take into account the 4f electron contribution. The same approximation (mdf) was adopted for the Cu atom. The standard all-electron 6-31G** basis was used for all remaining atoms.¹⁴ Geometry optimizations were performed using analytical gradient techniques.

EFISH Measurements. The molecular quadratic hyperpolarizability of the investigated complexes was measured by the solution phase direct current EFISH generation method in solution,¹⁵ which can provide direct information on the intrinsic molecular NLO properties through eq 1

$$\gamma_{\text{EFISH}} = (\mu\beta_{\lambda}/5kT) + \gamma(-2\omega; \omega, \omega, 0) \quad (1)$$

where $\mu\beta_{\lambda}/5kT$ is the dipolar orientational contribution, and $\gamma(-2\omega; \omega, \omega, 0)$ is the third-order polarizability corresponding to the mixing of two optical fields at ω and the dc poling field at $\omega = 0$. This latter term is usually referred to as the electronic cubic contribution to γ_{EFISH} , which is usually negligible. β_{λ} is the projection along the dipole moment axis of the vectorial component of the tensor of the quadratic hyperpolarizability at the incident wavelength λ . All EFISH measurements were carried out at the Dipartimento di Chimica of the Università degli Studi di Milano, working in CH₂Cl₂ solutions at a concentration of 3×10^{-4} M, with a nonresonant incident wavelength of 1.907 μm , obtained by Raman-shifting in a high pressure H₂ of the fundamental 1.064 μm wavelength produced by a Q-switched, mode-locked Nd³⁺:YAG laser manufactured by Atalaser. The apparatus used for EFISH measurements is a prototype made by SOPRA (France). The $\mu\beta_{\text{EFISH}}$ values reported are the mean values of 16 successive measurements performed on the same sample. The sign of $\mu\beta_{\lambda}$ is determined by comparison with the reference solvent (CH₂Cl₂).

HLS Measurements. The HLS technique¹⁶ involves the detection of the incoherently scattered second harmonic light generated by a solution of the molecule under irradiation with a laser of wavelength λ ,

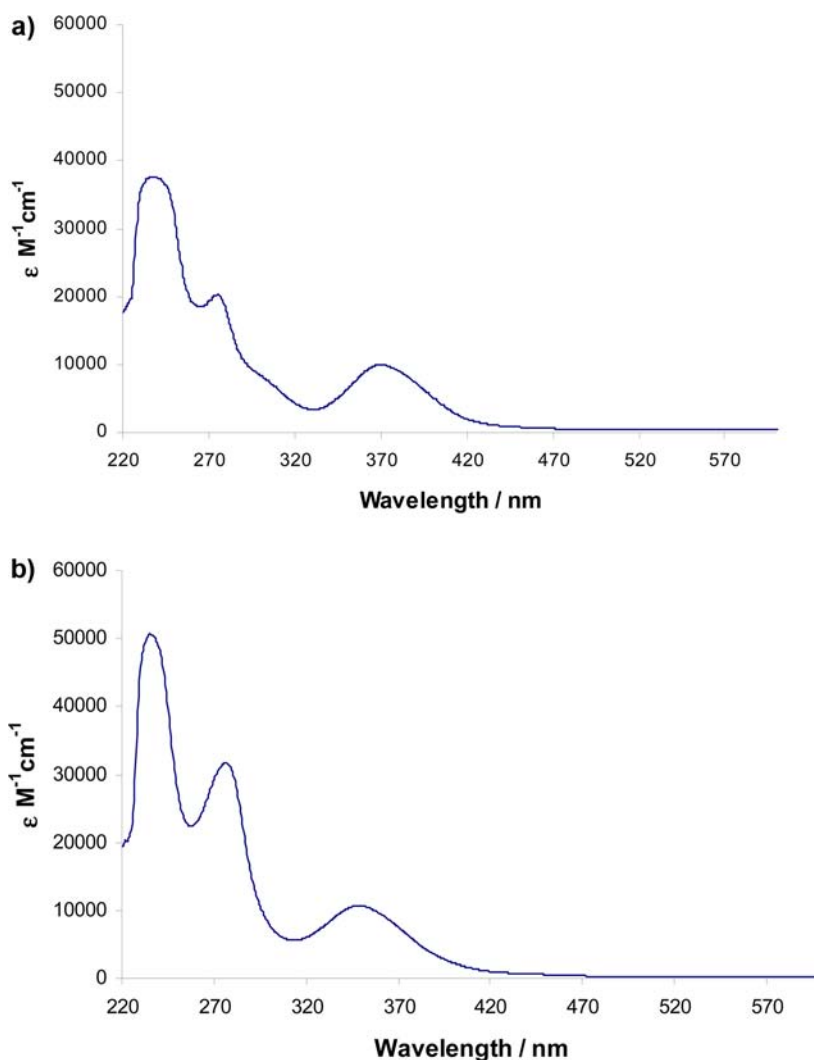


Figure 2. a. UV–vis spectrum of a CH_2Cl_2 solution of CuL. b. UV–vis spectrum of a CH_2Cl_2 solution of $[\text{Ce}(\text{NO}_3)_3(\text{CuL})_2]$.

leading to the measurement of the spatial average mean value of the $\beta \times \beta$ tensor product, $\langle \beta_{\text{HLS}} \rangle$. All HLS measurements were carried out at the École Normale Supérieure de Cachan in CH_2Cl_2 at a concentration of 3×10^{-4} M, working with a low energy nonresonant incident wavelength of $1.907 \mu\text{m}$, obtained as reported on the above description of EFISH measurements, then preventing from any parasitic contribution, such as 2-photon induced fluorescence, to the second harmonic signal.

X-ray Powder-Diffraction Data. X-ray diffraction data on powders were obtained on polycrystalline powders using a Philips PW1830 diffractometer, with graphite-monochromated $\text{CuK}\alpha$ radiation ($\lambda = 1.5405 \text{ \AA}$). The following data collection conditions were used: 2θ scan range $5\text{--}60^\circ$, step width 0.02° , time per step 10 s, divergence slit 0.25° , soller slit 0.04 rad , antiscatter slit 0.5° .

Synthesis of CuL (*N,N'*-1,3-Propylen-bis(salicylideneiminato)-copper(II)). The CuL complex was synthesized by dropwise adding, under stirring, 10 mL of a 28% ammonia solution to 50 mL of an ethanol (EtOH) solution containing 2.824 g (0.010 mol) of *N,N'*-bis(salicylidene)-2,2'-dimethyl-1,3-propanediamine. Then, 20 mL of a warm aqueous solution containing 1.345 g (0.010 mol) of CuCl_2 have been added dropwise under stirring. After a few minutes pale yellow-green crystals were obtained and left to digest at 60°C for three hours. Afterward, the suspension was left to cool to room temperature, and then the crystals were washed with cold ethanol and dried in air. Yield = 75%. Elemental analysis for $\text{C}_{17}\text{H}_{16}\text{CuN}_2\text{O}_2$: C = 59.38; H = 4.69; N = 8.15; Found: C = 59.58; H = 4.53; N = 8.15%. Exact mass of CuL = 343 (molecular weight = 343.87); MS (MALDI⁺, m/z fragments; M^* =

CuL: 344 ($M^* + \text{H}^+$), 366 ($M^* + \text{Na}^+$), 382 ($M^* + \text{K}^+$). IR (Nujol; ν/cm^{-1}): 1619 (s), 2680 (w). UV–vis in $\text{C}_2\text{H}_5\text{OH}$: 229.2 nm, 274.2 nm, 364.4 nm

General Synthesis of $[\text{Ln}(\text{NO}_3)_3(\text{CuL})_2]$. 2.00×10^{-3} mol of CuL were dissolved in 100 mL of EtOH at 70°C . Twenty-five mL of a warm (50°C) EtOH solution containing 1.00×10^{-3} mol of $\text{Ln}(\text{NO}_3)_3 \cdot 6\text{H}_2\text{O}$ have been dropwise added to the above solution under stirring. At the end of this addition a pale yellow-green precipitate appeared. The whole suspension was left to digest at 60°C for two hours. Afterward, the suspension was left to cool to room temperature, and the precipitate was filtered under vacuum and repeatedly washed using cold EtOH. For details see the Supporting Information.

Characterization of $[\text{La}(\text{NO}_3)_3(\text{CuL})_2]$. Elemental analysis for $\text{C}_{34}\text{H}_{32}\text{Cu}_2\text{LaN}_7\text{O}_{13}$: C = 40.33; H = 3.19; N = 9.68; Found: C = 40.32; H = 3.12; N = 9.56%. EDX Cu/La = 1.93. Exact mass of $[\text{La}(\text{NO}_3)_3(\text{CuL})_2] = 1011$ (molecular weight = 1012.65); MS (MALDI⁺, m/z fragments: $M^* = [\text{La}(\text{NO}_3)_3(\text{CuL})_2]$, 949 ($M^* - \text{NO}_3^-$), 1074 ($M^* + \text{Cu}^+$), IR (Nujol; ν/cm^{-1}): 1622 (s), 1550 (s), 1475 (s), 1280 (s), 1030 (m), 822 (m). UV–vis in $\text{C}_2\text{H}_5\text{OH}$: 226.4 nm, 273.4 nm, 362.2 nm.

Characterization of the Novel Complex $[\text{Ce}(\text{NO}_3)_3(\text{CuL})_2]$. Elemental analysis for $\text{C}_{34}\text{H}_{32}\text{Cu}_2\text{CeN}_7\text{O}_{13}$: C = 40.28; H = 3.18; N = 9.67; Found: C = 40.32; H = 3.12; N = 9.58%. EDX Cu/Ce = 1.91. Exact mass of $[(\text{CuL})_2\text{Ce}(\text{NO}_3)_3] = 1012$ (molecular weight = 1013.87); MS (MALDI⁺, m/z fragments: $M^* = [\text{Ce}(\text{NO}_3)_3(\text{CuL})_2]$, 950 ($M^* - \text{NO}_3^-$), 1075 ($M^* + \text{Cu}^+$). IR (Nujol; ν/cm^{-1}): 1620 (s),

Table 1. Electronic Absorption Spectra (λ_{\max} of the Bands Responsible of the Second-Order NLO Properties), Calculated Dipole Moments (μ), β_{EFISH} , (β_{HLS}), Dipolar and Octupolar Contributions to the Quadratic Hyperpolarizability of CuL and $[\text{Ln}(\text{NO}_3)_3(\text{CuL})_2]$ Complexes, Measured in CH_2Cl_2 Solution

		λ_{\max} (nm) [$\epsilon \text{ M}^{-1}\text{cm}^{-1}$]	$\mu\beta_{\text{EFISH}} \times 10^{-48}$ esu	$\mu \text{ D}$	$\beta_{\text{EFISH}}^a \times 10^{-30}$ esu	$\langle\beta_{\text{HLS}}\rangle^a \times 10^{-30}$ esu	$\ \beta^{(1)}\ \times 10^{-30}$ esu	$\ \beta^{(3)}\ ^b \times 10^{-30}$ esu
CuL	0	370 [10000]	210	5.31	40	510	31	1650
Ln	f electrons							
La	0	348 [5660]	350	9.54	37	520	29	1680
Ce	1	348 [10640]	400	6.60	61	540	47	1750
Sm	5	348 [11570]	600	7.32	82	560	64	1810
Eu	6	347 [8870]	720	7.01	103	610	80	1970
Er	11	347 [8490]	810	7.17	113	640	88	2070

^aThe error of EFISH and HLS measurements is $\pm 10\%$. ^bThe total quadratic hyperpolarizability $\|\beta\|$ (from eq 2) is essentially equal to $\|\beta^{(3)}\|$.

1552 (s), 1477 (s), 1280 (s), 1028 (m), 820 (m). UV–vis in $\text{C}_2\text{H}_5\text{OH}$: 227.5 nm, 274.0 nm, 361.5 nm.

Characterization of $[\text{Sm}(\text{NO}_3)_3(\text{CuL})_2]$. Elemental analysis for $\text{C}_{34}\text{H}_{32}\text{Cu}_2\text{SmN}_7\text{O}_{13}$: C = 39.88; H = 3.15; N = 9.57; Found: C = 40.03; H = 3.12; N = 9.35%. EDX Cu/Sm = 1.83. Exact mass of $[\text{Sm}(\text{NO}_3)_3(\text{CuL})_2] = 1024$ (molecular weight = 1024.11); MS (MALDI⁺, m/z fragments: $M^* = [\text{Sm}(\text{NO}_3)_3(\text{CuL})_2]$, 962 ($M^* - \text{NO}_3^-$). IR (Nujol; ν/cm^{-1}): 1622 (s), 1555 (s), 1475 (s), 1285 (s), 1030 (m), 822 (m). UV–vis in $\text{C}_2\text{H}_5\text{OH}$: 226.0 nm, 274.0 nm, 364.8 nm.

Characterization of $[\text{Eu}(\text{NO}_3)_3(\text{CuL})_2]$. Elemental analysis for $\text{C}_{34}\text{H}_{32}\text{Cu}_2\text{EuN}_7\text{O}_{13}$: C = 39.81; H = 3.14; N = 9.56; Found: C = 39.98; H = 3.12; N = 9.56%. EDX Cu/Eu = 1.92. Exact mass of $[\text{Eu}(\text{NO}_3)_3(\text{CuL})_2] = 1025$ (molecular weight = 1025.71); MS (MALDI⁺, m/z fragments: $M^* = [\text{Eu}(\text{NO}_3)_3(\text{CuL})_2]$, 963 ($M^* - \text{NO}_3^-$). IR (Nujol; ν/cm^{-1}): 1620 (s), 1560 (s), 1480 (s), 1285 (s), 1028 (m), 820 (m). UV–vis in $\text{C}_2\text{H}_5\text{OH}$: 226.6 nm, 273.0 nm, 364.4 nm.

Characterization of $[\text{Er}(\text{NO}_3)_3(\text{CuL})_2]$. Elemental analysis for $\text{C}_{34}\text{H}_{32}\text{Cu}_2\text{ErN}_7\text{O}_{13}$: C = 39.23; H = 3.01; N = 9.42; Found: C = 38.30; H = 2.99; N = 9.39%. EDX Cu/Er = 2.00. Exact mass of $[\text{Er}(\text{NO}_3)_3(\text{CuL})_2] = 1038$ (molecular weight = 1041.01); MS (MALDI⁺, m/z fragments: $M^* = [\text{Er}(\text{NO}_3)_3(\text{CuL})_2]$, 976 ($M^* - \text{NO}_3^-$). IR (Nujol; ν/cm^{-1}): 1618 (s), 1555 (s), 1480 (s), 1280 (s), 1030 (m), 820 (m). UV–vis in $\text{C}_2\text{H}_5\text{OH}$: 227.0 nm, 273.3 nm, 363.0 nm.

RESULTS AND DISCUSSION

Synthesis and Spectroscopic Characterization. The lanthanide complexes $[\text{Ln}(\text{NO}_3)_3(\text{CuL})_2]$ (Ln = La, Ce, Sm, Eu, Er; L = N,N'-1,3-propylen-bis(salicylideneiminato), with (CuL), coordinating to Ln ions as a bidentate ligand, have been prepared following a procedure reported for similar complexes.^{7a,b}

As a result of the lanthanide contraction, changes in coordination through the series may be expected. In fact, a trinuclear nature (2 Cu and 1 Ln) was hypothesized for La and Sm, whereas a dinuclear structure (1 Cu and 1 Ln: $[\text{Ln}(\text{NO}_3)_3(\text{CuL})_2] \cdot 2\text{H}_2\text{O}$) was presented for Eu and Er.^{7a}

In contrast, in the present work, all evidence points to trinuclear lanthanide systems (Ln = La, Ce, Sm, Eu, Er). In fact, elemental analysis, EDX measurements, and XRD patterns are indicative for $[\text{Ln}(\text{NO}_3)_3(\text{CuL})_2]$ systems, trinuclear and isomorphous, independently for the nature of the Ln ion.

XRD patterns show that all the complexes investigated in this work are isostructural with each other and have a trinuclear structure as that reported for the related complex $\{\text{Ce}(\text{NO}_3)_3[\text{Cu}(\text{salen})]_2\}$.¹⁷

Due to the low solubility of the complexes and their poorly crystalline nature it was not possible to obtain their single crystal X-ray structure.

A trinuclear system in the case of Er is remarkable, since a dinuclear structure was reported for $\{\text{Er}(\text{NO}_3)_3[\text{Cu}(\text{salen})]\}$.¹⁷

Figure 2a shows the electronic absorption spectrum of a solution of CuL in CH_2Cl_2 . Three bands at 230, 272, and 370 nm are present. The electronic absorption spectra of the $[\text{Ln}(\text{NO}_3)_3(\text{CuL})_2]$ complexes have a similar pattern although the band at lower energy is blue-shifted, by 22–23 nm, for Ln = La, Ce, Sm, and Eu (Figure 2 and Table 1). As reported in Figure 2b in the electronic absorption spectrum of a solution of $[\text{Ce}(\text{NO}_3)_3(\text{CuL})_2]$ in CH_2Cl_2 , the three bands are at 230, 276, and 347 nm, respectively. These electronic absorption spectra are consistent with bands associated with $\pi \rightarrow \pi^*$ transitions. The high energy bands (230–276 nm), identical for all $[\text{Ln}(\text{NO}_3)_3(\text{CuL})_2]$ (Ln = La, Ce, Sm, and Eu) complexes, arise from the phenyl rings, while the lower energy transition (348–370 nm) is due to the azomethine chromophore. The blue shift observed for the lower energy band, on going from CuL to $[\text{Ln}(\text{NO}_3)_3(\text{CuL})_2]$, is due to the complexation to the lanthanide ion.^{7a,c}

Dipole Moments and Second-Order NLO Properties.

The geometry of the structure of the lanthanide complexes $[\text{Ln}(\text{NO}_3)_3(\text{CuL})_2]$ have been optimized by DFT calculations (Figure 1 and Figure 3). The CuL ligands as well as two nitrate ligands are placed in equatorial positions around the metal

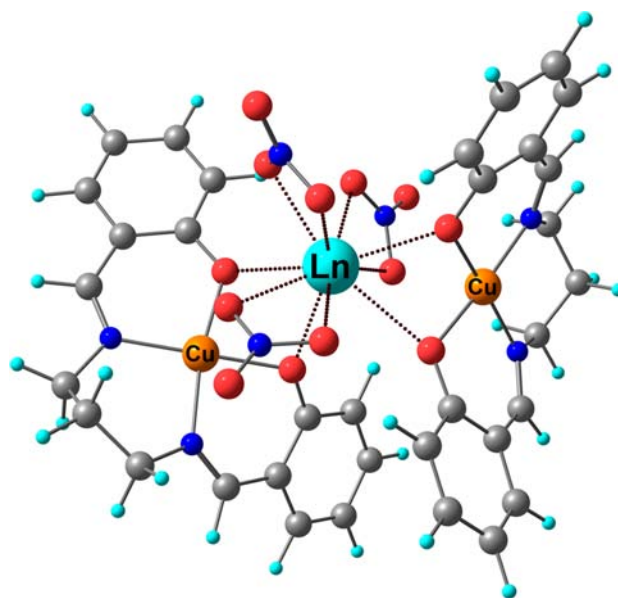


Figure 3. Structure obtained by DFT calculations of the $[\text{Ln}(\text{NO}_3)_3(\text{CuL})_2]$ complexes. Carbon in gray, oxygen in red, nitrogen in blue, hydrogen in light blue.

center. The remaining third nitrate group lies in the axial position approximately along the C_2 symmetry axis (Figure 3).

Geometrical parameters, in terms of distances between the metal center and the ligands, are similar in all the complexes. Only $[\text{La}(\text{NO}_3)_3(\text{CuL})_2]$ shows distances slightly increased (about +0.07 Å) compared to the other complexes. In particular, for the lanthanum complex, all the nitro groups show a geometrical arrangement in which two oxygens for each nitro group are involved in the coordination with the metal center. In all the other lanthanide complexes the nitro groups are similarly arranged, but one equatorial nitro group shows a geometrical arrangement in which only one oxygen atom is involved in the coordination with the metal center. N–O distances of each nitro group validate these considerations. In particular, N–O bonds involved in the coordination with the metal center are longer than the other N–O bonds of about 0.05 Å (see the Supporting Information for the details of the geometry coordinates). The larger coordination sphere of the lanthanum ion allows a more relaxed arrangement of the nitrate groups placed in equatorial position with respect to the other complexes. Dipole moments of all the complexes $[\text{Ln}(\text{NO}_3)_3(\text{CuL})_2]$ ($\text{Ln} = \text{La}, \text{Ce}, \text{Sm}, \text{Eu}, \text{and Er}$) were determined on the geometry-optimized structures using the DFT framework with an open shell approach. The calculated dipole moments lie along the C_2 axis for all the complexes. For complexes containing f electrons, the dipole moment values are very close to each other, ranging from 6.60 to 7.32 D. Only for the lanthanum complex (number of f electrons = 0) the calculated dipole moment increases to 9.54 D (see Table 1).

The different geometry arrangement of nitro groups observed in the lanthanum complex (as previously described) lead to a different spatial charge distribution that in turn can be adducted as the main factor responsible of the different dipole moment value found in the lanthanum complex with respect to the other lanthanide complexes.

The quadratic hyperpolarizability β_{EFISH} and $\langle\beta_{\text{HLS}}\rangle$ of all the complexes was determined in CH_2Cl_2 solution, working with a nonresonant incident radiation of low energy ($\lambda = 1.907 \mu\text{m}$), by a combination of HLS and EFISH techniques in order to evaluate both the dipolar and octupolar contributions and therefore to get a deep understanding of the origin of their second-order NLO properties (Table 1).

Complex $[\text{La}(\text{NO}_3)_3(\text{CuL})_2]$ is characterized by a relatively low value of β_{EFISH} , quite similar to that of CuL. A much higher value is obtained for $[\text{Ce}(\text{NO}_3)_3(\text{CuL})_2]$ with a further increase along the Ln series, confirming the previously reported effect of the presence and number of f electrons on the second-order NLO properties.^{3,6}

As reported in Table 1 and shown in Figure 4a, β_{EFISH} values initially increase rapidly with the number of f electrons, starting from lanthanum to europium; then the increase of β_{EFISH} is less marked upon addition of the other f electrons, since the β_{EFISH} value of the Er complex (11 f electrons) is only 1.1 times higher than that of the Eu complex (6 electrons). This trend is in agreement with that previously reported for β -diketonate diglyme lanthanide complexes.⁶

It must be pointed out that β_{EFISH} is related to the dipolar origin of the second-order NLO response since it represents the projection along the dipole moment axis of the vectorial component of the tensor describing the quadratic hyperpolarizability.

Therefore in order to have a complete understanding of the various components, dipolar and octupolar, of the second-order

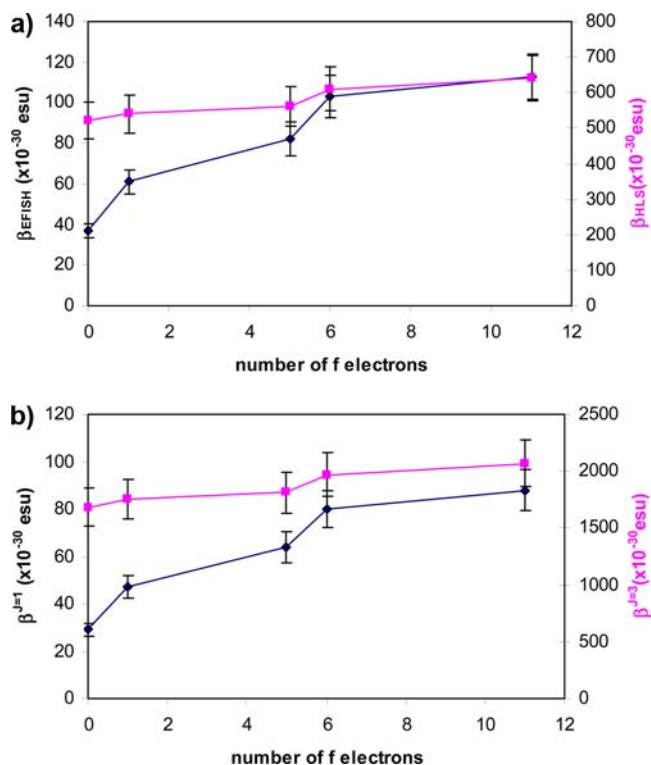


Figure 4. a. Dependence of β_{EFISH} ($\times 10^{-30}$ esu) and $\langle\beta_{\text{HLS}}\rangle$ ($\times 10^{-30}$ esu) upon the number of f electrons. b. Dependence of $\|\beta^{J=1}\|$ ($\times 10^{-30}$ esu) and $\|\beta^{J=3}\|$ ($\times 10^{-30}$ esu) upon the number of f electrons.

NLO properties of the Ln complexes investigated in this work, dipolar and octupolar contributions to the quadratic hyperpolarizability were obtained from an HLS investigation, working with a nonresonant incident wavelength of 1.907 μm . The dipolar ($J = 1$) and octupolar ($J = 3$) contributions and the modulus of the quadratic hyperpolarizability ($\|\beta\|$) have been calculated according to the following equations,^{16a,b} since all compounds have a C_{2v} symmetry.

$$\|\bar{\beta}\|^2 = \|\bar{\beta}^{J=1}\|^2 + \|\bar{\beta}^{J=3}\|^2 \quad (2)$$

$$\|\beta^{J=1}\| = \sqrt{\frac{3}{5}} \beta_{\text{EFISH}} \quad (3)$$

$$\begin{aligned} \langle\beta_{\text{HLS}}^2\rangle &= \langle\beta_{\text{XXX}}^2\rangle + \langle\beta_{\text{ZXX}}^2\rangle \\ &= \frac{2}{9} \|\bar{\beta}^{J=1}\|^2 + \frac{2}{21} \|\bar{\beta}^{J=3}\|^2 \end{aligned} \quad (4)$$

Remarkably, the various complexes are characterized by a significant quadratic hyperpolarizability $\langle\beta_{\text{HLS}}\rangle$ (510×10^{-30} – 640×10^{-30} esu), which increases relatively slowly but steadily with the number of f electrons, the enhancement factor from La to Er being about 1.2. This behavior is similar to that previously observed for $[\text{LLn}(\text{NO}_3)_3]$ ($\text{L} = \text{dibutylaminophenyl-function-alyzed annelated terpyridine}$)^{3d,e} and $[\text{Ln}(\text{hfac})_3(\text{diglyme})]$ ($\text{hfac} = \text{hexafluoroacetylacetonate}$; $\text{diglyme} = \text{bis}(2\text{-methoxyethyl})\text{ether}$)⁶ but is in contrast with that reported by Tanner, Wong et al.,^{3h} and Parker et al.,³ⁱ where the values of $\langle\beta_{\text{HLS}}\rangle$ reach a maximum around the center of the series. Why the latter systems differ so markedly in their behavior remains unclear.^{3h,i} As shown in Table 1, the high values of $\langle\beta_{\text{HLS}}\rangle$ of the complexes prepared in the present work are due to a high

octupolar $\|\beta^{f=3}\|$ component, the dipolar component $\|\beta^{f=1}\|$ being less than 4% of the octupolar one. Therefore, the quadratic hyperpolarizability $\|\beta\|$ (calculated from eq 2) is essentially equal to the octupolar component $\|\beta^{f=3}\|$. Such a high octupolar component is probably originated from a coordination sphere with a large π delocalization characterizing the CuL ligands. In fact, for other Ln complexes, with a coordination sphere much less rich of π delocalized ligands the dipolar contribution becomes much more significant.

However it is worth pointing out that also the quite small dipolar component $\|\beta^{f=1}\|$ is characterized, as β_{EFISH} , by a quite significant initial increase of its value with the number of f electrons (Table 1) starting from lanthanum to europium, followed by a less significant increase upon addition of other f electrons.

Since as pointed out above, $\|\beta^{f=3}\|$ corresponds quite completely with $\|\beta\|$, the effect of the increase of the number of f electrons is much less relevant (Table 1), thus confirming that the high value of $\|\beta^{f=3}\|$ is mainly related to the large π delocalization of the CuL ligands of the coordination sphere.

Interestingly, along the first half of the Ln series, the increase of $\|\beta^{f=3}\|$ is much lower than that of $\|\beta^{f=1}\|$, whereas a similar quite irrelevant increase is observed in the second half (Table 1 and Figure 4b).

It is important to emphasize the fact that both β_{EFISH} and $\langle\beta_{\text{HLS}}\rangle$ values of all complexes investigated in the present work are remarkably higher than those reported for β -diketonate diglyme lanthanide complexes,⁶ as expected from molecules containing more conjugated ligands.

CONCLUSION

In our work, the trinuclear nature of $[\text{Ln}(\text{NO}_3)_3(\text{CuL})_2]$ complexes has been put in evidence. They have been investigated by a combination of HLS and EFISH techniques in order to evaluate both the dipolar and octupolar contributions to their quite significant quadratic hyperpolarizability and to confirm that f electrons may tune their second-order NLO response. In the complexes investigated, the major contribution to the total quadratic hyperpolarizability is largely controlled by the octupolar contribution, but the values of both β_{EFISH} and $\|\beta^{f=1}\|$, that is the dipolar part, are significantly influenced by the number of f electrons, thus confirming that, as suggested,³⁸ the unexpected polarizable character of f electrons may be the origin of such fascinating evidence. Moreover we have also confirmed what has already been reported by some of us:⁶ the increase of the values of both β_{EFISH} and $\|\beta^{f=1}\|$ is significant up to fulfilment of half f shell, while it becomes much less relevant by addition of further f electrons up to the total fulfilment of the f shell. It appears thus that this is a general trend, whose origin is worth being investigated.

ASSOCIATED CONTENT

Supporting Information

Complete reference 11 and optimized geometries in Cartesian coordinates of the Ln complexes. This material is available free of charge via the Internet at <http://pubs.acs.org>.

AUTHOR INFORMATION

Corresponding Author

*E-mail: (C.D.) claudia.dragonetti@unimi.it. E-mail: (A.G.) agulino@dipchi.unict.it.

Notes

The authors declare no competing financial interest.

ACKNOWLEDGMENTS

This work was supported by MIUR (FIRB 2003: RBNE033K-MA, FIRB 2004: RBPR05JH2P and PRIN 2008: 2008FZK5AC_002) and by the Centro Nazionale delle Ricerche. We also acknowledge CINECA Award N. HP10CPZKOT 2012 for providing computing resources.

REFERENCES

- (1) For example, see (a) Kanis, D. R.; Lacroix, P. G.; Ratner, M. A.; Marks, T. J. *J. Am. Chem. Soc.* **1994**, *116*, 10089–10102. (b) Heck, J.; Dabek, S.; Meyer-Friedrichsen, T.; Wong, H. *Coord. Chem. Rev.* **1999**, *190–192*, 1217–1254. (c) Le Bozec, H.; Renouard, T. *Eur. J. Inorg. Chem.* **2000**, *2*, 229–239. (d) Lacroix, P. G. *Eur. J. Inorg. Chem.* **2001**, *2*, 339–348. (e) Di Bella, S. *Chem. Soc. Rev.* **2001**, *30*, 355–366. (f) Coe, B. J. In *Comprehensive Coordination Chemistry II*; McCleverty, J. A., Meyer, T. J., Eds.; Elsevier: Oxford, 2004; Vol. 9, pp 621–687. (g) Coe, B. J.; Curati, N. R. M. *Comments Inorg. Chem.* **2004**, *25*, 147–184. (h) Cariati, E.; Pizzotti, M.; Roberto, D.; Tessore, F.; Ugo, R. *Coord. Chem. Rev.* **2006**, *250*, 1210–1233. (i) Coe, B. J. *Acc. Chem. Res.* **2006**, *39*, 383–393. (j) Humphrey, M. G.; Samoc, M. *Adv. Organomet. Chem.* **2007**, *55*, 61–136. (l) Di Bella, S.; Dragonetti, C.; Pizzotti, M.; Roberto, D.; Tessore, F.; Ugo, R. In *Topics in Organometallic Chemistry 28. Molecular Organometallic Materials for Optics*; Le Bozec, H., Guerschais, V., Eds.; Springer: 2010; Vol. 28, pp 1–55. (m) Maury, O.; Le Bozec, H. In *Molecular Materials*; Bruce, D. W., O'Hare, D., Walton, R. I., Eds.; Wiley: Chichester, 2010; pp 1–59.
- (2) (a) Special Issue on Lanthanide Chemistry: *Chem. Rev.* **2002**, *102*, 1807–2476. (b) Jiang, X.; Jen, A. K. Y.; Huang, D.; Phelan, G. D.; Londergan, T. M.; Dalton, L. R. *Synth. Met.* **2002**, *125*, 331–336.
- (3) (a) Andraud, C.; Maury, O. *Eur. J. Inorg. Chem.* **2009**, 4357–4371. (b) Townsend, P. D.; Jazmati, A. K.; Karali, T.; Maghrabi, M.; Raymond, S. G.; Yang, B. J. *Phys.: Condens. Matter* **2001**, *13*, 2211–2224. (c) Bogani, L.; Cavigli, L.; Bernot, K.; Sessoli, R.; Gurioli, M.; Gatteschi, D. *J. Mater. Chem.* **2006**, *16*, 2587–2592. (d) Sénéchal, K.; Toupet, L.; Ledoux, I.; Zyss, J.; Le Bozec, H.; Maury, O. *Chem. Commun.* **2004**, 2180–2181. (e) Sénéchal-David, K.; Hemeryck, A.; Tancrez, N.; Toupet, L.; William, J. A. G.; Ledoux, I.; Zyss, J.; Boucekine, A.; Guégan, J. P.; Le Bozec, H.; Maury, O. *J. Am. Chem. Soc.* **2006**, *128*, 12243–12255. (f) Tancrez, N.; Feuvrie, C.; Ledoux, I.; Zyss, J.; Toupet, L.; Le Bozec, H.; Maury, O. *J. Am. Chem. Soc.* **2005**, *127*, 13474–13475. (g) Furet, E.; Costuas, K.; Rabiller, P.; Maury, O. *J. Am. Chem. Soc.* **2008**, *130*, 2180–2183. (h) Law, G.-L.; Wong, K.-L.; Lau, K.-K.; Lap, S.-t.; Tanner, P. A.; Kuo, F.; Wong, W.-T. *J. Mater. Chem.* **2010**, *20*, 4074–4079. (i) Walton, J. W.; Carr, R.; Evans, N. H.; Funk, A. M.; Kenwright, A. M.; Parker, D.; Yufit, D. S.; Botta, M.; De Pinto, S.; Wong, K.-L. *Inorg. Chem.* **2012**, *51*, 8042–8056.
- (4) (a) Roos, B. O.; Lindh, R.; Malmqvist, P.; Veryazov, V.; Widmark, P.-O.; Borin, A. C. *J. Phys. Chem. A* **2008**, *112*, 11431–11435. (b) Adamo, C.; Maldivi, P. *J. Phys. Chem. A* **1998**, *102*, 6812–6820. (c) Di Bella, S.; Gulino, A.; Lanza, G.; Fragala, I.; Stern, D.; Marks, T. J. *Organometallics* **1994**, *13*, 3810–3815.
- (5) (a) Gulino, A.; Di Bella, S.; Fragalà, I.; Casarin, M.; Seyam, A. M.; Marks, T. J. *Inorg. Chem.* **1993**, *32*, 3873–3879. (b) Gulino, A.; Casarin, M.; Conticello, V. P.; Gaudiello, J. G.; Mauermann, H.; Fragalà, I.; Marks, T. J. *Organometallics* **1988**, *7*, 2360–2364. (c) Fragalà, I. L.; Gulino, A. In *Fundamental and Technological Aspects of Organo-f-Elements Chemistry: Photoelectron Spectroscopy of f-Element Organometallic Complexes*; Marks, T. J., Fragalà, I. L., Eds.; NATO ASI-Reidel Publishing Company: 1985; pp 327–360.
- (6) Valore, A.; Cariati, E.; Righetto, S.; Roberto, D.; Tessore, F.; Ugo, R.; Fragalà, I. L.; Fragalà, M. E.; Malandrino, G.; De Angelis, F.; Belassi, L.; Ledoux-Rak, I.; Thi, K. H.; Zyss, J. *J. Am. Chem. Soc.* **2010**, *132*, 4966–4970.
- (7) (a) Condorelli, G.; Fragalà, I.; Giuffrida, S.; Cassol, A. Z. *Anorg. Allg. Chem.* **1975**, *412*, 251–257. (b) Harrison, D. W.; Bünzli, J.-C. G.

Inorg. Chim. Acta **1985**, *109*, 185–192. (c) Welby, J.; Rusere, L. N.; Tanski, J. M.; Tyler, L. A. *Inorg. Chim. Acta* **2009**, *362*, 1405–1411.

(8) See for example: (a) Cristovao, B.; Mirosław, B.; Klak, J. *Polyhedron* **2012**, *34* (1), 121–128. (b) Chandrasekhar, V.; Senapati, T.; Dey, A.; Das, S.; Kalisz, M.; Clerac, R. *Inorg. Chem.* **2012**, *51* (4), 2031–2038. (c) Hu, S.; Sheng, T.; Wen, Y.; Fu, R.; Wu, X. *Inorg. Chem. Commun.* **2012**, *16*, 28–32. (d) Kajiwara, T.; Nakano, M.; Takahashi, K.; Takaiishi, S.; Yamashita, M. *Chem.-A Eur. J.* **2011**, *17* (1), 196–205, S196/1–S196/3. (e) Pasatoiu, T. D.; Madalan, A. M.; Zamfirescu, M.; Tiseanu, C.; Andruh, M. *Phys. Chem. Chem. Phys.* **2012**, *14*, 11448–11456.

(9) (a) Di Bella, S.; Fragalà, I.; Ledoux, I.; Diaz-Garcia, M. A.; Marks, T. J. *J. Am. Chem. Soc.* **1997**, *119*, 9550–9557. (b) Di Bella, S.; Fragalà, I.; Ledoux, I.; Marks, T. J. *J. Am. Chem. Soc.* **1995**, *117*, 9481–9485. (c) Di Bella, S.; Fragalà, I.; Ledoux, I.; Diaz-Garcia, M. A.; Lacroix, P. G.; Marks, T. J. *Chem. Mater.* **1994**, *6*, 881–883. (d) Di Bella, S.; Fragalà, I. *Synth. Met.* **2000**, *115*, 191–196.

(10) Di Bella, S.; Oliveri, I. P.; Colombo, A.; Dragonetti, C.; Righetto, S.; Roberto, D. *Dalton Trans.* **2012**, *41*, 7013–7016.

(11) Frisch, M. J. et al. *Gaussian 09*, Revision C.01; Gaussian, Inc.: Wallingford, CT, 2009.

(12) Perdew, J. P.; Burke, K.; Ernzerhof, M. *Phys. Rev. Lett.* **1996**, *77*, 3865–68.

(13) (a) Dolg, M.; Stoll, H.; Savin, A.; Preuss, H. *Theor. Chim. Acta* **1989**, *75*, 173–194. (b) Dolg, M.; Stoll, H.; Preuss, H. *J. Chem. Phys.* **1989**, *90*, 1730–1734.

(14) (a) Hehre, W. J.; Ditchfield, R.; Pople, J. A. *J. Chem. Phys.* **1972**, *56*, 2257–2261. (b) Francl, M. M.; Pietro, W. J.; Hehre, W. J.; Binkley, J. S.; Gordon, M. S.; DeFrees, D. J.; Pople, J. A. *J. Chem. Phys.* **1982**, *77*, 3654–3665.

(15) Ledoux, I.; Zyss, J. *Chem. Phys.* **1982**, *73*, 203–213.

(16) (a) Zyss, J. *Chem. Phys.* **1993**, *98*, 6583–6599. (b) Brasselet, S.; Zyss, J. *J. Opt. Soc. Am. B* **1998**, *15*, 257–288. (c) Maker, P. D. *Phys. Rev. A* **1970**, *1*, 923–951. (d) Clays, K.; Persoons, A. *Phys. Rev. Lett.* **1991**, *66*, 2980–2983. (e) Zyss, J.; Ledoux, I. *Chem. Rev.* **1994**, *94*, 77–105.

(17) Kahn, M. L.; Rajendiran, T. M.; Jeannin, Y.; Mathonière, C.; Kahn, O. C. *R. Acad. Sci. Paris, Sér. IIc, Chimie/Chem.* **2000**, *3*, 131–137.